Unstable Flow during Redistribution: Controlling Factors and Practical Implications

Zhi Wang*, William A. Jury, Atac Tuli, and Dong-Ju Kim

Zhi Wang, Department of Earth and Environmental Sciences, California State University, Fresno, CA 93740. * Corresponding email address (zwang@csufresno.edu).

William A. Jury and Atac Tuli, Department of Environmental Sciences, University of California, Riverside, CA 92521.

Dong-Ju Kim, Dept. of Environmental Geosphere Science, Korea University, Seoul, Republic of Korea.

Unstable Flow during Redistribution: Controlling Factors and Practical Implications

Zhi Wang*, William A. Jury, Atac Tuli, and Dong-Ju Kim

Abstract: Unstable flow causes major uncertainties in the characterization of drainage in the vadose zone by inducing finger-like flow paths in soils with or without macropores. Recent studies have identified the major factors governing fingered flow to be the combined effects of capillary hysteresis, the existence of a threshold water-entry value in a porous medium and a positive matric potential gradient behind the wetting front. This situation typically occurs during redistribution following high-rate infiltration - a common occurrence in hydrology. The conditions favoring instability can also develop during infiltration into a fine-over-coarse layered soil, into hydrophobic or air-entrapped soils, or even in a homogeneous coarse-textured soil if the infiltration rate is low. An analysis of the conditions necessary for the onset of unstable flow in a uniform soil is provided in this paper. We demonstrate that if the matric potential gradient (*dh/dz*) becomes positive during redistribution, a perturbation at the wetting front will cause finger flow. However, if *dh/dz* remains negative, the perturbation will be dissipated. The analysis is used to predict a critical depth of irrigation (I_c) beyond which the flow should become unstable. A series of point-source and line-source infiltration experiments were conducted using a slab-box filled with uniform sands. The results confirmed that as soon as I_c is exceeded a finger was formed at the bottom of the wetting front, channeling the flow and stopping water movement in the surrounding areas. The implications of this phenomenon for practical irrigation and leaching designs are discussed.

1. Introduction

Unstable flow was originally discovered in petroleum engineering as viscous-driven fingering during horizontal and upward water-oil displacement, and its characteristics were described by linear stability theory (Saffman and Taylor, 1958; Chuoke et al., 1959). When the theory was applied to downward flow in the vadose zone, Hill and Parlange (1972) found that the gravity-driven fingering occurs when the infiltration flux i falls below the saturated hydraulic conductivity K_s. Based on the derivation of Chuoke et al. (1959) and accounting for the stabilizing effects of soil capillarity, Wang et al. (1998c) predicted that fingering should occur over a narrower range of flux ratio (i/K_s) and primarily in coarse-textured soils. Numerous experimental studies over the past three decades have confirmed that unstable flow occurs under a number of soil and hydraulic conditions. The most widely recognized conditions for unstable flow are: vertical flow from a fine-textured layer into a coarse one (Hill and Parlange, 1972; Parlange and Hill, 1976; Starr et al., 1978, 1986; Glass et al., 1988, 1989a,b; Baker and Hillel, 1990; Nieber, 1996); infiltration into a hydrophobic medium (van Ommen et al., 1988; Hendrickx et al., 1993; Ritsema et al., 1993; Nguyen et al., 1999; Carrillo et al., 2000; Wang et al., 2000b); soil air compression during infiltration (White et al., 1976, 1977; Wang et al., 1997, 1998a,c); and unsaturated infiltration under low application rates (Selker et al., 1992; Yao and Hendrickx, 1996; Wang et al., 1998b; Geiger and Durnford, 2000). In addition to these recognized situations, another condition predicted to cause unstable flow in uniform porous media is redistribution following the cessation of infiltration (Raats, 1973; Philip, 1975). Diment and Watson (1985) and Tamai et al. (1987) demonstrated that redistribution causes unstable flow in coarse-textured uniform materials that were oven dry. However, Diment and Watson's (1985) experiments in a small slab box showed that redistribution "stabilized" when the initial water

content was increased to only a few percent of saturation. In contrast, recent experiments of Wang et al. (2003a,b) in the field and a large slab box showed that redistribution is unstable even in a very wet uniform sand. Nicholl et al. (1994) observed fingering during redistribution in initially dry fractures. Based on an analysis of these results, Jury et al. (2003) made the conjecture that water flow is unstable to different degrees in every soil because of redistribution -- an almost unavoidable scenario in hydrology.

The common mechanism driving unstable flow in soil under all of these conditions seems to be the combined effects of capillary hysteresis, the existence of a threshold water-entry value of the porous medium and a positive matric potential gradient (dryer toward the surface) behind the wetting front (Jury et al., 2003). It is well known that the matric potential becomes more negative toward the surface as infiltration shifts to redistribution (Youngs, 1958ab). Thus the transition from infiltration to redistribution creates the very condition necessary for unstable flow.

Many previous field experiments that involved repeated infiltration/drainage cycles have observed a breakup of the wetting front into narrow fingers (Jury et al., 1986; Glass et al., 1988; Kung, 1990; Ghodrati and Jury, 1992; Flury et al., 1994). These results may have been influenced by redistribution, since some period of time elapsed prior to excavation and exposure of the wetting front. It becomes clear that flow uncertainties in the subsurface are sometimes dominated by the occurrence of unstable flow in both heterogeneous and homogeneous porous media.

Unstable channeling of water into fingers in the surface zone potentially creates many problems for water and chemical management. Management of water for crop production becomes more wasteful. Fertilizers and pesticides can move quickly below the depth where they

are needed. Chemical waste can migrate much deeper than predicted on the basis of uniform movement. In addition, management strategies devised on the basis of stable flow to optimize water and chemical use might not be optimum in the presence of unstable flow.

The objectives of this study are: 1) to identify and quantify the critical factors triggering unstable flow during redistribution after a certain amount of infiltration; 2) to determine whether an optimum amount of irrigation or rainfall will minimize or eliminate unstable flow; and 3) to conduct experiments to validate the predictions made by our analysis.

2. Theoretical Considerations

Early investigations of redistribution dealt primarily with the determination of field capacity (Alway and McDole, 1917; Veihmeyer and Hendrickson, 1931; Colman, 1944) which has long been accepted as an operational physical property of soil (Jury et al., 1991). Field capacity is by definition the amount of water remaining in surface storage after redistribution has become insignificant. However, the possibility of fingered flow during redistribution obscures this definition, and raises questions about its' utility.

2.1. One Dimensional Redistribution

Infiltration and redistribution are generally regarded as one dimensional unless the water supply is not spatially uniform. Once capillary hysteresis was detected and reported by Haines (1930), it became clear that infiltration and redistribution required different methods of analysis. In the years following, many studies were conducted to conceptually separate redistribution from infiltration (Childs and Collis-George, 1950; Youngs, 1958a, b; Nielsen et al., 1962; Biswas et al., 1966; Gardner et al., 1970; Poulovassillis, 1970; Talsma, 1974). However, most experimental and theoretical investigations of redistribution assumed one-dimensional flow in a uniform

porous medium (Gardner, 1959; Staple, 1966; Rubin, 1967) with continued advance of the wetting front during both infiltration and redistribution. However, due to difficulties in defining the initial conditions and representing the physics of hysteresis at the Darcy scale, the redistribution process remains less well understood than infiltration despite considerable effort (Philip, 1991).

In an important but largely overlooked study, Youngs (1958a,b) showed that the shape of the soil moisture profile during redistribution was not necessarily the same as that of infiltration. To explain the differing moisture profiles during redistribution, Peck (1971) conceptualized that at each depth during redistribution, the moisture content increases to a maximum then decreases. Thus, when the maximum water content value is at $z = z^*$ (*the transition plane*), the soil is drying in the upper zone $0 \leq z \leq z^*$ and is wetting in the lower region $z > z^*$. In a subsequent analysis, Youngs and Poulovassilis (1976) identified two forms of redistribution profile. In the first, the moisture profile shape remains similar to that of infiltration - maintaining the highest water content at the soil surface and the lowest at the wetting front (Fig. 1a). In the second, the transition plane occurs at an intermediate depth between the surface and the wetting front, at a location corresponding to the depth reached at the end of infiltration (Fig. 1b). Youngs and Poulovassilis explained that these two types of profile had different rates of redistribution.

However, apart from the two forms of redistribution discussed by Youngs and Poulovassilis (1976), there was clearly a third profile shape shown in Fig. 2 of Youngs (1958b), and redrawn in Fig 1c here, in which the moisture content is highest at the moving wetting front and decreases monotonically to the soil surface. This third form of redistribution profile has not been explained previously in the literature. It can be inferred from recent studies that the third form of redistribution illustrates that a threshold water-entry pressure at the wetting front is

required for water to enter the unwetted zone (see Hillel and Baker, 1988; Baker and Hillel, 1990; Selker et al., 1992; Liu et al., 1993, 1994; Geiger and Durnford, 2000). In this case water content is at its highest value at the front.

2.2. Relative Dominance of Capillary versus Gravity Forces

If water infiltrates relatively uniformly during infiltration of an amount of water I, the front will extend to a depth (L) in the soil given approximately by

$$L = \frac{I}{q_a - q_i} \qquad (1)$$

where q_a is the average moisture content in the wetted zone ($0 < z < L$) and q_i is the initial moisture content. Figure 2a shows typical wetting and drying matric potential-water content curves for a coarse-textured soil with a narrow range of pore sizes during the transition from infiltration to redistribution. As shown by Peck (1971), the soil below the transition plane $z = z^*$ initially takes up moisture following a wetting curve OA until the moisture content reaches a maximum value (q^*) at $z = z^*$, as shown in Fig. 2a. When the water potential reaches the water-entry value h_{we} at the wetting front, the water content increases abruptly to q_{we} (Point A). Above the transition plane, water drains from the soil following the drainage curve BO (Fig. 2a). When the potential falls to the air-entry value h_{ae} (Point C), the major pores will begin to empty. Hence, the difference between the water- and air-entry values indicates the ability of a porous medium to hold a suspended vertical water column against gravity (Fig. 2b) or entrap a zone of higher water content behind the wetting front (Fig. 2d). This special moisture retention ability of a porous medium can be defined as the *capillary suspension length* (S):

$$S = \frac{h_{we} - h_{ae}}{\cos b} \qquad (2)$$

where b is the direction (or slope) of flow with respect to gravity. This equation was first conceived by Glass et al. (1989a) to describe the length of the "saturated" finger tip in vertical flow (b=0); it was later used by Nicholl et al. (1994) to describe the mechanisms governing redistribution in a single fracture. It will be shown in the following that the relative magnitudes of L and S determine whether finger flow will occur.

When $L < S = h_{we} - h_{ae,}$ as shown in Fig. 2b (for b =0), downward flux, $i = -KG$, is not possible unless the total pressure gradient $G = (h_A - L - h_B)/L$ is ≤ 0 or $h_B = h_A - L$. Here, K is the hydraulic conductivity of the porous medium, h_B is the matric potential at the soil surface (point B) and $h_A = h_{we}$ is the matric potential at the wetting front (point A). Thus, for $L = S = h_{we} - h_{ae}$, h_B must be greater than the air-entry value of the soil. For $L < S$, h_B must be even greater to maintain a downward flow. In the early stages following the cessation of water application, $h_B > h_{ae}$, the flow of water is downward and L increases. However, h_B will eventually fall to a value $h_{ae}+(S - L)$ before L exceeds S and flow will stop, leaving the profile suspended in space. This situation will produce a sequence of matric potential profiles as shown in Fig. 3a. The corresponding moisture profile will be the first form of redistribution as shown in Fig. 1a.

When a larger amount of infiltration occurs such that $L > S$ (Fig.2c), downward flow continues after water input stops, because the matric potential h_B at the surface is above the air-entry value and the matric potential head gradient across the wetted zone between the surface and the front $G_m = (h_{we} - h_B)/L \leq 1$. In this case, downward flow will still occur even after the surface potential is reduced below the air-entry value because $L > h_{we} - h_{ae}$. Hence, drainage can start from the surface. Once air enters the soil near the surface, the moisture profile will trap a wetted zone of water from the point C in the profile where $h = h_{ae}$ to point A where $h = h_{we}$ at the wetting front (Fig. 2d). In order to maintain continued downward flow through this region,

the elevation difference between A and C should be greater than S (i.e. $G_m \leq 1$). This should produce a series of matric potential profiles, $h = h(z,t)$, as shown in Fig. 3b. The corresponding moisture profiles, $q = q(z,t)$, will display the third form of redistribution (Fig. 1c).

Thus, the shape of the redistribution profile is a direct consequence of hysteresis and the interplay of gravitational (downward) and capillary (upward) forces at the end of infiltration. When capillary forces dominate (i.e. $L \leq S$) at the end of infiltration then by Eqs. (1) and (2)

$$I \leq \frac{(h_{we} - h_{ae})(q_a - q_i)}{\cos b} \tag{3}$$

In this case there is insufficient suction produced by the downward flow to induce drainage of the large pores near the surface. In contrast, when the gravitational force dominates the flow (i.e. $L > S$), then

$$I > \frac{(h_{we} - h_{ae})(q_a - q_i)}{\cos b} \tag{4}$$

In this case, sufficient suction will be generated by the downward flow to induce drainage at the soil surface first, so that an intermediate zone of high water content will be formed behind the moving wetting front during redistribution. The length of this zone is equal to the *capillary suspension length* (S). Since the water-entry value (h_{we}) decreases as initial water content q_i increases (Smith, 1967; Liu et al., 1994; Wang et al., 2003a), the blob is longer in relatively moist soils than in dry soils.

2.3. Horizontal and Inclined Redistribution

Horizontal redistribution ($b = 90°$) should produce a capillary-dominated moisture profile (Fig. 1a) because gravitational potential differences are absent and the right hand side of Eq. (3) becomes infinite. Experimental evidence of this behavior can be seen in Nielsen et al. (1962) and Youngs and Poulovassilis (1976). For inclined redistribution, Youngs and Poulovassilis (1976)

showed that for the same amount of water application (I = 3.24 cm), the redistribution profiles changed from gravity-dominated (Fig. 1b or c) to capillary-dominated (Fig. 1a) when the soil column angle of tilt was changed from $b \leq 60°$ to $b \geq 75°$. Their results also showed the water content near the source of application increased as b increased.

2.4. Finger Flow in Two- or Three-dimensional Frames

As shown in Figures 3a and 3b, the matric potential gradient $\partial h/\partial z$ behind the front was initially negative during saturated infiltration, then changed to positive during redistribution. If the system flux, i, is governed by Darcy's law (with depth z positive downward)

$$i = K_{we}\left(1 - \frac{\partial h}{\partial z}\right) \qquad (5)$$

a positive gradient ($\partial h/\partial z > 0$) means that the flux rate becomes less than the water-entry conductivity of the porous medium ($i < K_{we}$). Because the wetting front moves only when h is greater than the water-entry value h_{we}, the flux condition $i < K_{we}$ results in a channeling of the wetting front into a narrower area (occupied by fingers) that still conducts a total flux of $i = K_{we}$.

In one-dimensional experiments conducted in narrow columns, fingers cannot develop when there is insufficient cross-sectional area (Wang et al., 2003a). However, the wetting front in this case may still become inclined, "tongue like" or wavy, depending on column diameter, soil texture and initial moisture content (Peck, 1965; White et al., 1976, 1977; Diment and Watson, 1985). Apparently, the column cross-section must be able to accommodate at least one unstable wavelength, which is approximately equal to twice the finger diameter (Chuoke et al., 1959). Many laboratory experiments fail to meet this criterion.

A 10-cm diameter cylindrical column containing coarse-textured soil manifested finger flow due to soil water redistribution even without air compression. A single large finger down

the center of the column was frozen and photographed by Wang et al. (2003a). In the column experiments of Youngs (1958b), the second type of moisture profile (Fig.1b) was reported, implying a positive matric potential gradient in the transmission zone. Youngs measured the average water content across the entire column cross section using thermal elements embedded in the soil. It is thus quite possible that the flow he observed was unstable, since the lower values of water content measured below the initial depth of wetting might have included high values of moisture inside the fingers and extremely low values outside.

Assuming that during the early stages of unstable flow the water flow in the fingers moves at a flux rate approximately equal to $K(h_{we})= K_{we}$ of the porous medium and the flow in the surrounding areas ceases, the water flow rate from the total cross sectional area A_s is equal to that in the fingered area A_f, i.e., $iA_s = K_{we} A_f$. It follows from Eq. (5) that the fingered flow area fraction, $F = A_f/A_s = i/K_{we}$, is equal to

$$F = 1 - \frac{\partial h}{\partial z} \qquad (6)$$

Hence, the likelihood of forming fingers is directly related to the magnitude of the positive matric potential gradient. For capillary-driven redistribution (Figs.1a and 3a), positive gradients are not possible unless upward flow occurs due to evaporation; therefore instability will not occur. However, gravity-dominated redistribution produces positive matric potential gradients and can be very unstable resulting in fingers in the porous medium (Figs. 1c and 4b).

2.5. Explanation of the Initiation of Unstable Flow

A physical argument can be used to illustrate why the direction of the matric potential gradient determines whether flow will be unstable. Suppose that a small-scale perturbation develops at the center of the wetting front during a surface-saturated infiltration event, causing the wetting front at that point to move slightly below the depth of wetting of the main profile

(Fig. 4a). Since the matric potential at the wetting front remains at the threshold water-entry value h_{we} (Jury et al., 2003), the perturbation causes a downward shift of the matric potential profile above it. When the matric potential increases toward the surface, as in saturated infiltration, the perturbation produces a *horizontal diverging flow* away from the center (solid thick line with an arrow) to the outside toward the dashed lines, as shown by the horizontal arrows, thereby eliminating the growth of the perturbation. However, during redistribution with the matric potential decreases toward the surface (Fig. 4b), the perturbation produces a *horizontal converging flow* toward the central thick line (finger), which depletes the surrounding matrix and promotes the growth of the perturbation. The white dotted arrow lines indicate the finger's capturing zone, above the lines the flow is considerably unsaturated. Because in this case the horizontal converging flow decreases the matric potential of the soil adjacent to the finger, the pressure at the wetting front of the soil zone may drop below the water-entry value, thereby preventing further downward movement outside of the fingers (Jury et al., 2003).

3. Experimental Validation

Previous experiments have confirmed that: (1) the wetting front does not move until the matric potential at the wetting front exceeds the water-entry value (h_{we}) of the porous medium (Hillel and Baker, 1988; Baker and Hillel, 1990); (2) the water potential at the moving wetting front stays at h_{we} (Selker et al., 1992; Liu et al., 1994; Geiger and Durnford, 2000); and (3) the absolute value of h_{we} (negative for wettable soils) increases with an increase in the initial water content, producing larger fingers in the porous medium (Smith, 1967; Liu et al., 1994; Wang et al., 2003a). Our experiments here were designed to validate that unstable flow will start during redistribution after Eq. (4) is satisfied, and that fingered flow will start sooner in coarse or dry

soils than in fine or wet soils. If Eq. (4) is valid, it is possible to select an appropriate amount of irrigation that will prevent or promote finger flow.

3.1. Experimental Materials and Methods

A sieved coarse silica sand (0.5 - 0.8 mm particle size, bounding US standard sieves 35 and 60) and a finer silica sand (0.25-0.5 mm size, bounding sieves 60 and140) were used in the experiments. The data for the drying retention curves of the sands are shown in Fig. 5 along with lines representing the best fit to the van Genuchten equation (1980):

$$q = q_r + (q_s - q_r)[1 + a(-h)^n]^{-m} \qquad (7)$$

where m=1-1/n. The physical properties of the sands and the optimized equation parameters are shown in Table 1. The water-entry values (h_{we}) of the coarser and finer sands (-6.8 and -11.7 cm respectively) were calculated using the empirical formula (h_{we}=4.37/d+0.07) of Baker and Hillel (1990), where d (mm) is the median particle size. Baker and Hillel found that measured water-entry values using the capillary-rise method were very close to the inflectional pressure heads (i.e., $h_{inf}=(1+m)^{-m}$) calculated using the van Genuchten model for the wetting retention curve. We used the drainage parameters and estimated the air-entry values to be h_{ae}= -12.6 cm for the coarser sand and h_{ae}= -19.0 cm for the finer sand. It can be seen from Fig.5 that although the optimized retention curves using RETC (van Genuchten, 1991) did not fit very well to the data from the coarse textured sands, the inflectional pressures were close to the air-entry values at the water contents near saturation. Hillel and Baker (1988) considered that the entry values are actually characteristic of an assemblage of pores, determined by the narrowest or largest pores that form a continuous network in the matrix. Therefore, the entry values do not necessarily correspond to the saturated water content. They can be directly measured using tension-pressure infiltrometers (Fallow and Elrick, 1998; Wang et al., 2000a).

The sands were uniformly packed into a large slab box with transparent walls (100 x 100 cm^2 plexiglass with 1-cm spacing) for visual observation of water flow. The exact packing procedures were described by Wang et al. (2003a). Because micro-roughness of the sand surface or a slight tilt of the slab-box will considerably affect the infiltration uniformity if an immediate ponding device was used, we designed a constant-speed moving applicator system to add water to the surface. A Marriott bottle (see Cutler, 1959) was connected to an adjustable irrigation dropper or a supply tube as a point source. A motor-driven cart was constructed to let travel along a pair of track rails installed above the slab box. An electronic relay system and two end-switches were installed on the cart so that it can move bi-directionally at a constant speed. The cart was carrying the Marriott bottle and a supply tube which provided a uniform flow as a "line" source. The travel speed of the cart was 100 cm per 15 s (a return travel takes 30 s) and the Marriott supply rate was 2 ml s^{-1}, thus resulting in a supply rate of 1080 cm h^{-1} which immediately created a ponded layer of water near the supply tube. The saturated hydraulic conductivity of the finer sand was 209 cm h^{-1}, and that of the coarser sand was 504 cm h^{-1}, see Table 1. The sand surface experienced a few seconds in an unponded but saturated condition during the moving-source application cycles.

Three sets of experiments were carried out. In the first, a 22-cm layer of the finer sand was packed over 70 cm of the coarser sand, and different amounts of water were supplied to the left and right half of the surface to produce a systematic variation in the depth of wetting. The purpose of this study was to observe the stability of the wetting front when it was less than or greater than the critical depth of wetting *S*. In the second experiment, only the coarser sand was packed into the slab box, and three different point-source applications were supplied at different locations along the surface. The first application of tap water was supplied instantaneously at the

middle of the surface using a funnel, while the second and third applications were added simultaneously at two points lateral to the surface. One of these point sources consisted of salty water (NaCl solution of density = 1.06 g cm^{-3}) and the other point was de-aired water (density = 0.992 g cm^{-3}). The purpose of this experiment was to observe the effects of supply rate and fluid density on finger propagation in the coarser sand.

In the third experiment, also conducted in the coarser sand, five irrigation and redistribution cycles were repeated over the whole input surface using the line-source water application. The first irrigation was insufficient to reach the critical depth of wetting, while later irrigations added sufficient water to exceed the depth. The background coarse sand was mostly wet; however, the top 10-cm layer was air dry. The purpose of this experiment was to observe unstable flow during repeated cycles of irrigation and redistribution in relation to the critical depth of irrigation. The detailed designs and flow parameters of all experiments are listed in Table 2.

3.2 Experimental Results

The critical depth of wetting (S) at the end of infiltration

The *capillary suspension length* (S) as defined by Eq. (2) is the critical depth of wetting at the end of infiltration that is predicted to cause unstable flow during redistribution. In Experiment 1, the top 22-cm finer sand has a water-entry value $h_{we} \tilde{}$ -12 cm and an air-entry value $h_{ae} \tilde{}$ -19 cm (Table 1), and therefore its critical wetting depth $S \tilde{}$ 7 cm. The first, non-uniform irrigation in Experiment 1 resulted in uneven wetting depths as shown in Fig. 6a (Irrigation I = 18 mm over the left half of the slab box, and I = 30 mm over the right half). Notice that the wetting depths at the start of redistribution (t = 0) varied from L = 5 cm ($L < S$) at the left

end of the frame to 9 cm ($L > S$) at the right end. As shown in Figs. 6b and 6c, the redistribution flow was stable and "frozen" on the left side when $L < S$. However, after reaching the critical depth of wetting ($L > S$) on the right side, the front became unstable and produced two fingers that penetrated deep into the profile. The finger fronts were temporarily impeded at the textural interface for about 15 min while pressure built up, then continued into the coarser layer. After the second uniform irrigation (I = 24 mm) over the entire surface, the wetting depths uniformly increased to $L>S$, as shown in Fig. 6d. Water on the right half of the profile was funneled into the old fingers, whereas water front on the left half also became unstable at one point producing a single finger which eventually reached the bottom of the frame (Figs. 6e and f). An additional finger emerged in the coarser layer between the previously generated fingers.

Unstable flow in the coarse sand under point-source irrigation

The point-source irrigations in Experiment 2 were supplied in two different ways. In the first irrigation, 150 ml of de-aired water was rapidly released through a funnel in 5 s, which created an initial wetting depth L that was clearly greater than the 5.8-cm critical depth of wetting in this coarse sand. The redistribution was clearly unstable as shown in Fig. 7a, creating a dominant gravity finger that extended to the bottom of the frame. In the second irrigation, the lighter de-aired water and heavier salty water were released simultaneously as drip irrigation (1 drop per second) at two separate points, causing unsaturated infiltration (the application rate was about 6 ml min^{-1}, equivalent to 360 cm h^{-1} over an effective 1 cm^2 wetted area, compared to K_s = 504 cm h^{-1} for the coarser sand). The wetting front first paused at the critical depth $L = S$ leaving a slightly enlarged area, then became fingered as shown in Figs. 7b-d. The salty and de-aired water fingers moved at the same speed and produced the same amount of drainage. Therefore,

the elevated fluid density did not affect finger flow in this case. The elevated density could be counteracted by the decrease in surface tension of the salty water.

Unstable flow in coarse sand under repeated line-source irrigation

Repeated irrigations are standard under field conditions. In Experiments 3, the entire surface received a sequence of irrigations (I = 6, 6, 6, 12, 24 mm at 0, 12, 24, 48, 49 and 72 hours, respectively. See Table 2). As shown in Fig. 8, fingers were produced during the second 6-mm irrigation, implying that the S value of this study was quite small. Additional fingers were produced during redistribution from subsequent irrigations. The repeated irrigation and drainage cycles did not effectively wet the top layer because the newly applied water was carried to the deeper layers through the old fingers.

4. Concluding Remarks

Our analyses have shown that the processes of infiltration and redistribution are qualitatively different in that the former can be simulated using traditional models; however, the latter is not predictable if the mechanisms of hysteresis and unstable flow are not considered.

A critical depth of wetting (S) was defined based on soil hysteresis. Thus, when the actual depth of wetting (L) is smaller than S, the infiltrated water stays near the surface. Otherwise, when $L > S$, finger flow will occur due to a positive matric potential gradient developed during redistribution. Our experimental results confirm this prediction.

Our laboratory experiments using dry and pre-wetted coarse sands supported the theoretical predictions. However, field conditions will be at least quantitatively different. Generally, less water will be stored in dry and coarse soils than in wet and fine ones, primarily due to increased redistribution instability in the former. Therefore, irrigation in coarse and dry

soils is not efficient even with point-source applications. Repeated water applications in coarse soils that have become unstable will only result in increased deep percolation through the fingers, and will not advance the water front in the matrix. Finger flow can be more effectively prevented in fine and wet soils which have large gaps between the water-entry and air-entry values, or larger critical wetting depths.

Acknowledgements: The research was supported by Research Grant No. IS-2859-97 from BARD, the US-Israel Binational Agricultural Research and Development Fund. Appreciation is expressed to the Associate Editor and two reviewers for their constructive suggestions.

References:

Alway, F.J., and G.R. McDole. 1917. Relation of the water retaining capacity of a soil to its hydroscopic coefficient. J. Agric. Res. 9:27-71.

Baker, R.S., and D. Hillel. 1990. Laboratory tests of a theory of fingering during infiltration into layered soils. Soil Sci. Soc. Am. J. 54:20-30.

Biswas, T.D., D.R. Nielsen, and J.W. Biggar. 1966. Redistribution of soil water after infiltration. Water Resour. Res. 2:513-524.

Carrillo, M.L.K., J. Letey, and S.R. Yates. 2000. Unstable water flow in a layered soil: I. Effects of stable water-repellent layer. Soil Sci. Soc. Am. J. 64:450-455.

Childs, E.C., and N. Collis-George. 1950. The permeability of porous media. Proc. Roy. Soc. London, 201A:392-405.

Chuoke, R.L., P. van Meurs, and C. van der Poel. 1959. The instability of slow, immiscible, viscous liquid-liquid displacements in permeable media. Tran. Am. Inst. Min. Metall. Pet. Eng. 216:188-194.

Colman, E.A. 1944. The dependence of field capacity upon depth of wetting of field soils. Soil Sci. 58:43-50.

Cutler, W.G., 1959, Constant rate of flow apparatus: American Journal of Physics, v. 17, no. 3, p. 185.

Diment, G.A., and K.K. Watson. 1985. Stability analysis of water movement in unsaturated porous materials, 3: Experimental studies. Water Resour. Res. 21:979-984.

Fallow, D.J., and D.E. Elrick. 1996. Field measurement of air-entry and water-entry soil water pressure heads, Soil Sci. Soc. Am. J. 60, 1036-1039.

Flury M., Fluhler H., Jury W.A., and J. Leuenberger. 1994. Susceptibility of soils to preferential flow of water: A field study. Water Resour. Res. 30:1945-1954.

Gardner, W.R. 1959. Solutions of the flow equation for the drying of soils and other porous media. Soil Sci. Soc. Am. Proc. 23:183-187.

Gardner, W. R., D. Hillel, and Y. Benyamini. 1970. Post-irrigation movement of soil water. 1. Redistribution. Water Resour. Res. 6:851-861.

Geiger, S.L., and D.S. Durnford. 2000. Infiltration in homogeneous sands and a mechanistic model of unstable flow., Soil Sci. Soc. Am. J. 64:460-469.

Ghodrati, M., and W.A. Jury. 1992. A field study of the effects of soil structure and irrigation method on preferential flow of pesticides in unsaturated soil. J. Contam. Hydrol. 11:101-125.

Glass, R.J., T.S. Steenhuis, and J.Y. Parlange. 1988. Wetting front instability as a rapid and far-reaching hydrologic process in the vadose zone. J. Contam. Hydrol. 3:207-226.

Glass R. J., Steenhuis T. S., and J. Y. Parlange, 1989a. Mechanism for finger persistence in homogeneous, unsaturated, porous-media - theory and verification. Soil Sci. 148:60-70.

Glass, R.J., T.S. Steenhuis, and J.Y. Parlange. 1989b. Wetting front instability, 2. Experimental determination of relationships between system parameters and two dimensional unstable flow field behavior in initially dry porous media. Water Resour. Res. 25:1195-1207.

Haines, W.B. 1930. Studies in the physical properties of soils: V. The hysteresis effect in capillary properties and the modes of moisture distribution associated therewith. J. Agric. Sci. 20:97-116.

Hendrickx, J.M.H., L.W. Dekker, and O.H. Boersma. 1993. Unstable wetting fronts in water repellent field soils. J. Environ. Qual. 22:109-118.

Hill, D.E., and J.Y. Parlange. 1972. Wetting front instability in layered soils. Soil Sci. Soc. Am. Proc. 36:697-702.

Hillel, D., and R.S. Baker. 1988. A descriptive theory of fingering during infiltration into layered soils, Soil Sci. 146:51-56.

Jury, W.A., H. Elabd, and M. Resketo. 1986. Field study of napropamide through unsaturated soil. Water Resour. Res. 5:749-755.

Jury, W. A., W. R. Gardner, and W. H. Gardner. 1991. Soil Physics, 5th Edition, John Wiley and Sons, New York.

Jury, W.A., Z. Wang, and A. Tuli. 2003. A conceptual model of unstable flow in unsaturated soil during redistribution, Vadose Zone J. 2:61-67.

Kung, K.J.S. 1990. Preferential flow in a sandy vadose zone, 1. Field observations. Geoderma 46:51-58.

Liu, Y., B.R. Bierck, J.S. Selker, T.S. Steenhuis, and J.Y. Parlange. 1993. High density X-ray and tensiometer measurements in rapidly changing preferential flow fields. Soil Sci. Soc. Am. J. 57:1188-1192.

Liu, Y., T.S. Steenhuis, and J.Y. Parlange. 1994. Formation and persistence of fingered flow fields in coarse grained soils under different moisture contents. J. Hydrol. 159:187-195.

Nguyen, H.V., JL. Nieber, C.J. Ritsema, L.W. Dekker, and T.S. Steenhuis. 1999. Modeling gravity driven unstable flow in a water repellent soil. J. Hydrol. 215:202-214.

Nicholl, M.J., R.J. Glass, and S.W. Wheatcraft. 1994. Gravity-driven infiltration instability in initially dry nonhorizontal fractures. Water Resour. Res. 30:2553-2546.

Nieber, J.L. 1996. Modeling finger development and persistence in initially dry porous media, Geoderma 70: 207-229.

Nielsen, D.R., J.W. Biggar, and J.M. Davidson. 1962. Experimental consideration of diffusion analysis in unsaturated flow problems. Soil Sci. Soc. Am. Proc. 2:107-111.

Parlange, J.Y., and D.E. Hill. 1976. Theoretical analysis of wetting front instability in soils. Soil Sci. 122:236-239.

Peck A.J. 1965. Moisture profile development and air compression during water uptake by bounded porous bodies: 3. Vertical columns. Soil Sci. 100: 44-51.

Peck., A.J. 1971. Redistribution of soil water after infiltration. Aust. J. Soil Res. 9: 59-71.

Philip J.R. 1975. Stability analysis of infiltration. Soil Sci. Soc. Am. Proc. 39:1042-1049.

Philip, J. R. 1991. Horizontal redistribution with capillary hysteresis. Water Resour. Res. 27:1459-1469.

Poulovassillis, A. 1970. Hysteresis of pore water in granular porous bodies. Soil Sci. 109:5-12.

Raats, P.A.C. 1973. Unstable wetting fronts in uniform and non-uniform soils. Soil Sci. Soc. Am. Proc. 37:681-685.

Ritsema C.J., L.W. Dekker, J.M.H. Hendrickx, and W. Hamminga. 1993. Preferential flow mechanism in a water repellent sandy soil. Water Resour. Res. 29:2183-2193.

Rubin, J. 1967. Numerical method for analysing hysteresis-affected, post-infiltration redistribution of soil moisture. Proc. Soil Sci. Soc. Am. 31:13-20.

Saffman, P.G. and S.G. Taylor. 1958. The penetration of fluid into a porous medium or Hele-Shaw cell containing a more viscous liquid. Proc. Roy. Soc. A., 245, 312-329, 1958.

Selker J.S, T.S. Steenhuis, and J.Y. Parlange. 1992. Wetting front instability in homogeneous sandy soils under continuous infiltration. Soil Sci. Soc. Am. J. 56:1346-1350.

Smith, W.O. 1967. Infiltration in sand and its relation to groundwater recharge. Water Resour. Res. 3: 539-555.

Staple, W.J. 1966. Infiltration and redistribution of water in vertical columns of loam soil. Soil Sci. Soc. Am. Proc. 30: 553-558.

Starr J.L., H.C. DeRoo, C.R. Frink, and J.Y. Parlange. 1978. Leaching characteristics of a layered field soil. Soil Sci. Soc. Am. J. 42:386-391.

Starr J.L., J.Y. Parlange, and C.R. Frink. 1986. Water and chloride movement through a layered field soil. Soil Sci. Soc. Am. J. 50:1384-1390.

Talsma, T. 1974. The effect of initial moisture content and infiltration quantity on redistribution of soil

water. Aust. J. Soil Res. 12:15-26.

Tamai, N., T. Asaeda, and C.G. Jeevaraj. 1987. Fingering in two-dimensional, homogeneous, unsaturated porous media. Soil Sci. 144:107-112.

van Ommen, H.C., L.W. Dekker, R. Dijksma, J. Hulsof, and W.H. van der Molen. 1988. A new technique for evaluating the presence of preferential flow paths in nonstructured soils. Soil Sci. Soc. Am. J. 52:1192-1193.

van Genuchten, M. Th. 1980. A closed form equation for predicting the hydraulic conductivity of unsaturated soils. Soil Sci. Soc. Am. J. 44:892-898.

van Genuchten, M. Th., F. J. Leij and S. R. Yates. 1991. The RETC code for quantifying the hydraulic functions of unsaturated soils, U.S. Salinity laboratory, USDA, ARS, Riverside, California, 1991.

Veihmeyer, F.J., and A.H. Hendrickson. 1931. The moisture equivalent as a measure of the field capacity of soils. Soil Sci. 32:181-193.

Wang, Z., J. Feyen, D.R. Nielsen, and M. Th. van Genuchten. 1997. Two-phase flow infiltration equations accounting for air entrapment effects. Water Resour. Res. 33:2759-2767.

Wang, Z., J. Feyen, M. Th. van Genuchten, and D.R. Nielsen. 1998a. Air entrapment effects on infiltration rate and flow instability. Water Resour. Res. 34:213-222.

Wang, Z., J. Feyen, and C.J. Ritsema. 1998b. Susceptibility and predictability of conditions for preferential flow. Water Resour. Res. 34:2169-2182.

Wang, Z., J. Feyen, and D.E. Elrick. 1998c. Prediction of fingering in porous media. Water Resour. Res. 34:2183-2190.

Wang, Z., L. Wu, and Q. J. Wu, 2000a. Water-entry value as an alternative indicator of soil water repellency and wettability, J. of Hydrology, 231-232: 76-83.

Wang, Z., Q.J. Wu, L. Wu, C.J. Ritsema, L.W. Dekker, and J. Feyen. 2000b. Effects of soil water repellency on infiltration rate and flow instability. J. Hydrol. 231-232:265-276.

Wang, Z, A. Tuli, and W.A. Jury. 2003a. Unstable flow during redistribution in homogeneous soil, Vadose Zone J. 2:52-60.

Wang, Z., L. Wu, T. Harter, J. Lu, and W.A. Jury. 2003b. A field study of unstable preferential flow

during soil water redistribution. Water Resour. Res. Vol. 39 No. 4. 10.1029/2001WR000903.

White, I., P.M. Colombera, and J.R. Philip. 1976. Experimental Studies of wetting front instability induced by sudden changes of pressure gradient. Soil Sci. Soc. Am. Proc. 40:824-829.

White, I., P.M. Colombera, and J.R. Philip. 1977. Experimental Studies of wetting front instability induced by gradual changes of pressure gradient and by heterogeneous porous media. Soil Sci. Soc. Am. Proc. 41:483-489.

Yao, T.-M., and J.M.H.Hendrickx. 1996. Stability of wetting fronts in dry homogeneous soils under low infiltration rates. Soil Sci. Soc. Am. J. 60:20-28.

Youngs, E.G. 1958a. Redistribution of moisture in porous materials after infiltration, 1. Soil Sci. 86:117-125.

Youngs, E.G. 1958b. Redistribution of moisture in porous materials after infiltration, 2. Soil Sci. 86:202-207.

Youngs, E.G., and A. Poulovassillis. 1976. The different forms of moisture profile development during the redistribution of soil water after infiltration. Water Resour. Res. 12:1007-1012.

Figure Captions:

Fig.1. Types of possible redistribution profile after ponded infiltration.

Fig.2. Schematics of moisture and pressure redistribution with respect to the amount of initial application: (a) hysteresis effects, (b) $L<S$, (c) $L>S$, and (d) water blob at the front. The asterisked variable indicates the maximum water content of the profile during redistribution (Peck, 1971).

Fig.3. Schematic matric potential profiles, $h = h(z, t)$, at the end of infiltration (t = 0) and at different times t during redistribution: (a) $L<S$, and (b) $L>S$. The asterisked variables indicate the positions of the maximum water content at the time (Peck, 1971).

Fig.4. Evolution of a perturbation at the wetting front during (a) ponded infiltration and (b) redistribution. The arrows show the flow directions.

Fig.5. Drying retention curves of the experimental materials.

Fig.6. Redistribution of unevenly applied water in a finer sand (top 22 cm) and a coarser sand (below) through a line-source. Symbols I and t denote the depth of water applied into the sands and the time of redistribution, respectively.

Fig.7. Redistribution of fluids in the coarse sand: (a) de-aired water (r = 0.993) added instantaneously; (b) through (d) salty water with anionic red dye (r = 1.06) and de-aired water through an irrigation dropper (1 drop per second or 6.6 ml min^{-1}). Symbols I and t denote the total amount (depth) of water applied and the time of redistribution, respectively.

Fig.8. Redistribution profiles of water in the wet coarse sand with repeated irrigation cycles. The top 10-cm sand was air-dry.

Table 1. Physical properties of the experimental material.

Material	Particle size	Saturated conductivity	Bulk density	Total porosity	Optimized van Genuchten Parameters				Threshold entry values §	
	d	K_s	r_b	f	q_r	q_s	a	n	h_{we}	h_{ae}
	mm	cm h^{-1}	g cm^{-3}	cm^3 cm^{-3}	cm^3 cm^{-3}	cm^3 cm^{-3}	cm^{-1}		cm	cm
Coarser sand	0.5-0.8	504	1.590	0.388	0.039	0.371	0.078	7.17	-6.8	-12.6
Finer sand	0.25-0.5	209	1.604	0.383	0.052	0.366	0.052	8.53	-11.7	-19.0

§ The air-entry pressure was set equal to the inflection point of the drying retention curve (Wang et al., 1997) and the water-entry pressure h_{we} was calculated using the empirical formula of Baker and Hillel (1990).

Table 2. Experimental designs and flow parameters.

Exp.	Material	Fluid supply	Critical wetting depth S
1 (Fig.6)	Dry finer sand (22-cm thick) over dry coarse sand (70-cm).	De-aired water, line-source. First irrigation non-uniform (I = 18 mm along the left 50-cm of the sand surface and I = 30 mm along the right 50-cm). Second irrigation uniform (I = 24 mm). Application rate = 12 mm/min.	7.3 cm
2 (Fig.7)	Dry coarser sand (92-cm high).	First irrigation instantaneously applied. Second irrigation supplied salty water with anionic red dye (r = 1.060 g cm^{-3}) and de-aired water (r = 0.993 g cm^{-3}); Point-source application rate = 6.6 ml min^{-1}. Total volume = 150 ml.	5.8 cm
3 (Fig.8)	Wet coarser sand with the top 10-cm layer air-dry.	De-aired water, line-source and 5 repeated Irrigations: I = 6 mm at 0 h, 6 mm at 24 h, 6 mm at 48 h, 12 mm at 49h and 24 mm at 72 h. Application rate: 12 mm min^{-1}.	< 5.8 cm for the top layer.

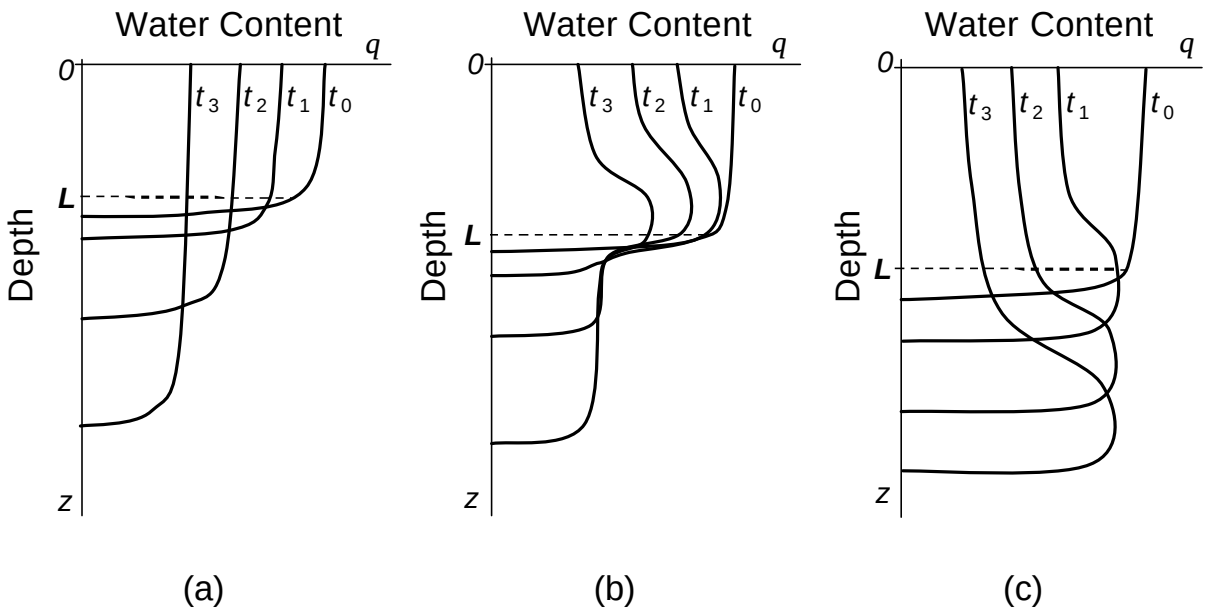

Fig. 1. Types of possible redistribution profile after ponded infiltration.

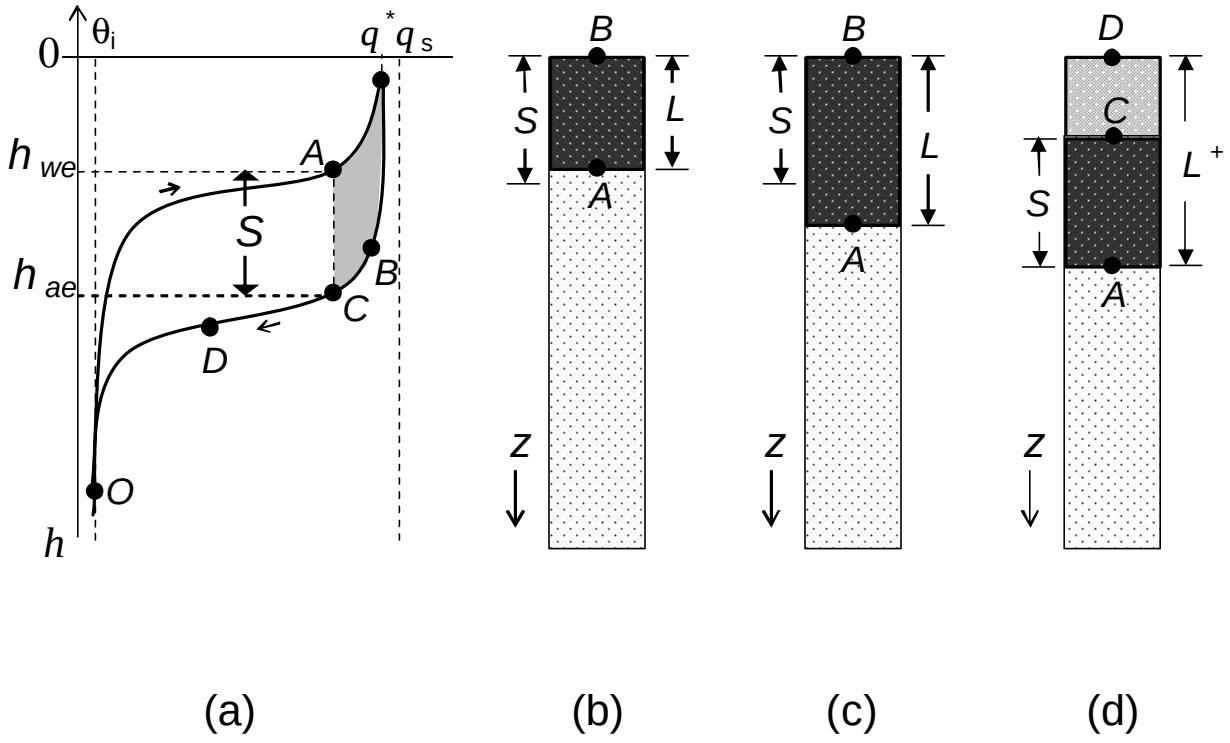

Fig. 2 Schematics of moisture and pressure redistribution with respect to the amount of initial application: (a) hysteresis effects, (b) $L<S$, (c) $L>S$, and (d) water blob at the front. The asterisked variable indicates the maximum water content of the profile during Redistribution (Peck, 1971).

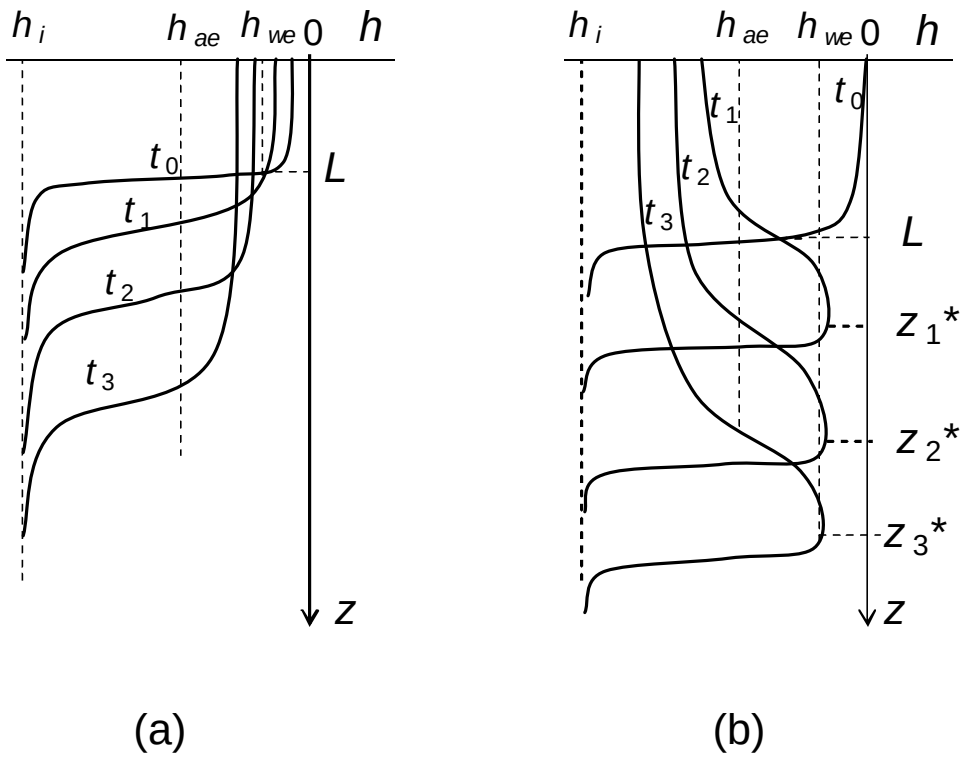

Fig. 3 Schematic matric potential profiles, $h = h(z, t)$, at the end of infiltration ($t = 0$) and at different times t during redistribution: (a) $L<S$, and (b) $L>S$. The asterisked variables indicate the maximum water content of the profile at the time (Peck, 1971).

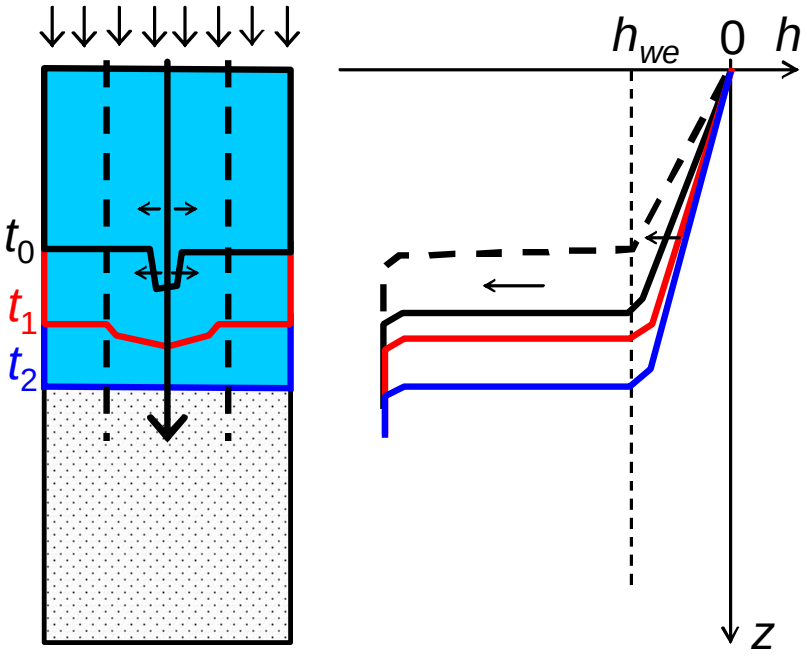

(a)

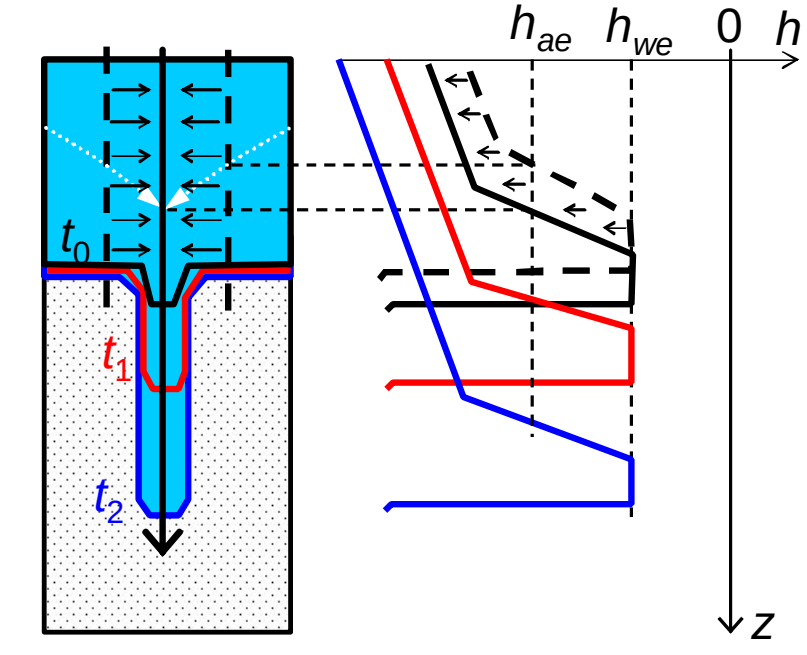

(b)

Fig. 4 Evolution of a perturbation at the wetting front during: (a) ponded infiltration and (b) redistribution or unsaturated infiltration. The arrows show the flow directions.

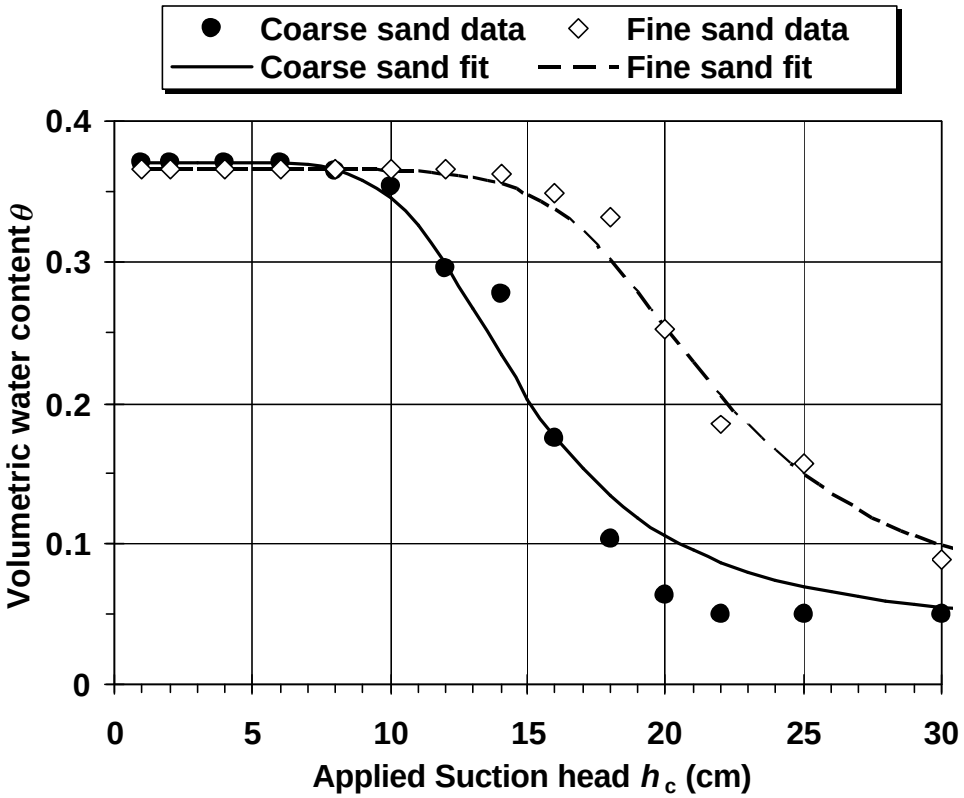

Fig. 5 Drying retention curves of the experimental materials.

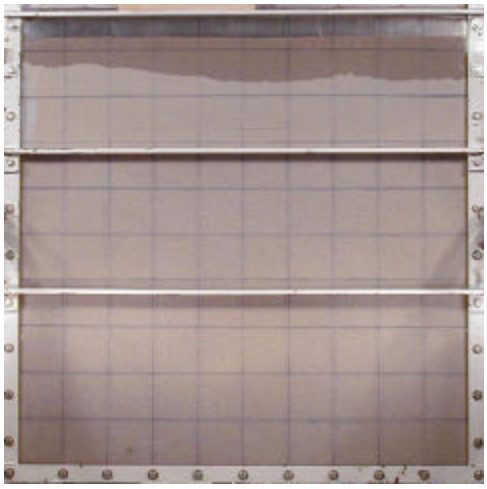

(a) 1st irrigation, *I* = 18~30 mm, *t* = 0 min

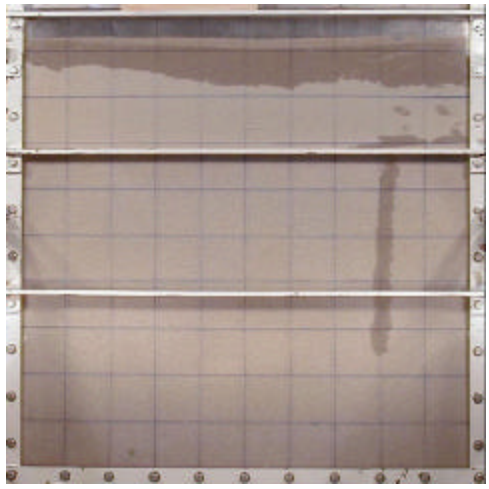

(b) 1st irrigation, *I* = 18~30 mm, *t* = 14 min

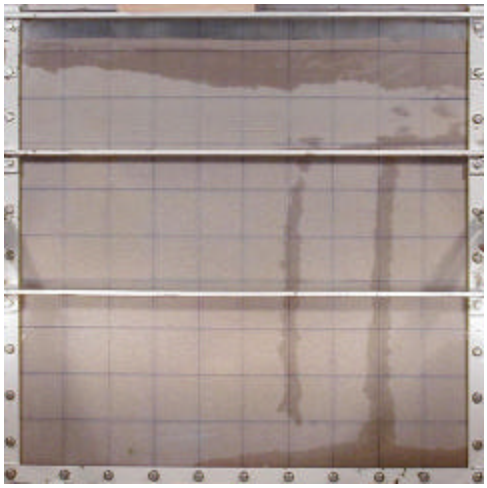

(c) 1st irrigation, *I* = 18~30 mm, *t* = 42 min

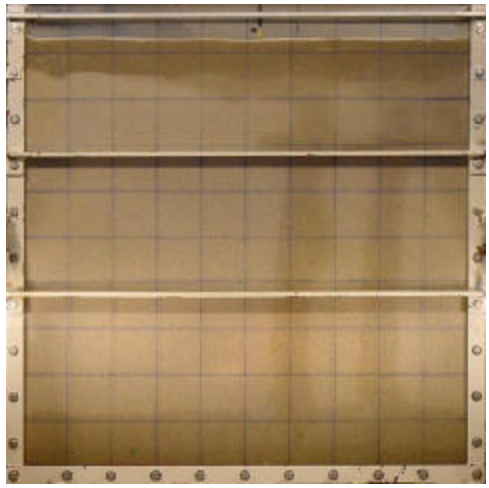

(d) 2nd irrigation, *I* = 24 mm, *t* = 0 min

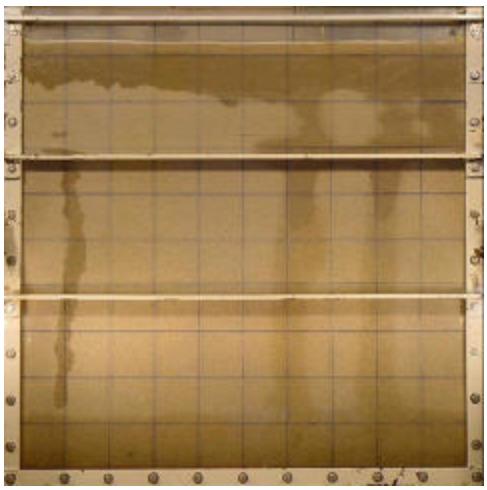

(e) 2nd irrigation, *I* = 24mm, *t* = 15 min

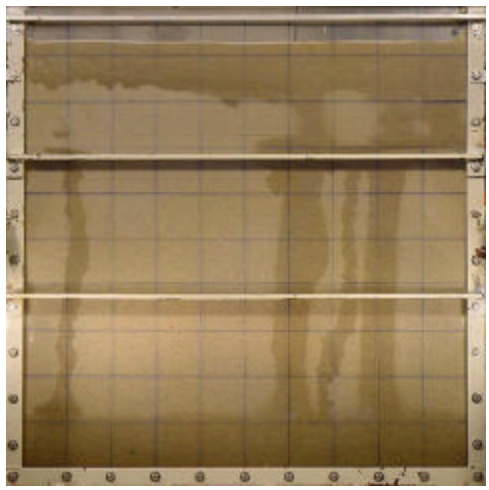

(f) 2nd irrigation, *I* = 24 mm, *t* = 70 min

Fig. 6 Redistribution of unevenly applied water in a fine sand (top 22 cm) and a coarse sand (below) through a line-source. Symbols *I* and *t* denote the depth of water applied into the sands and the time of redistribution, respectively.

(a) 1st irrigation, *I* = 150 ml, *t* = 20 min

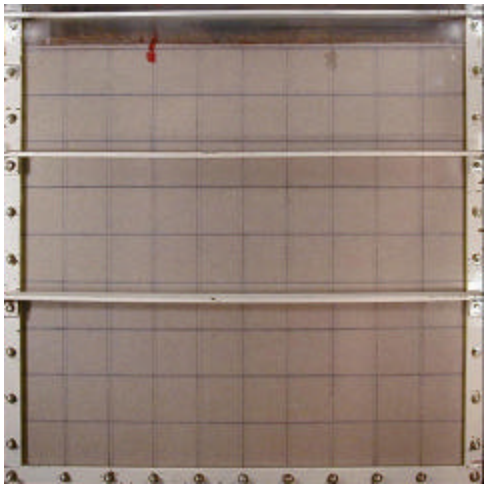

(b) 2nd irrigation, *I* = 1000 ml, *t* = 0.1 min

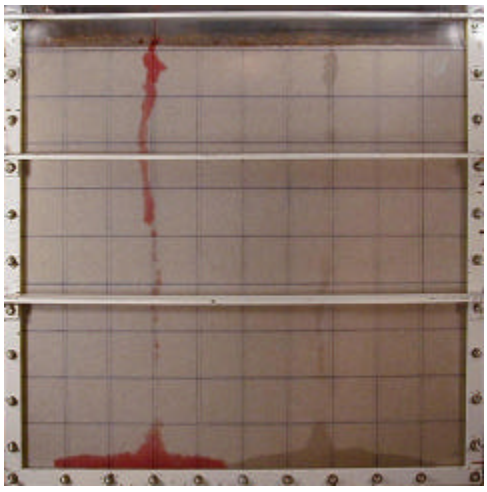

(c) 2nd irrigation, *I* = 1000 ml, *t* = 27 min

(d) 2nd irrigation, *I* = 1000 ml, *t* = 34 min

Fig. 7 Redistribution of fluids in the coarse sand: (a) de-aired water (ρ = 0.993) added instantaneously; (b) through (d) salty water with anionic red dye (ρ = 1.06) and de-aired water through an irrigation dropper (1 drop per second or 6.6 ml min-1). Symbols *I* and *t* denote the total amount (depth) of water applied and the time of redistribution, respectively.

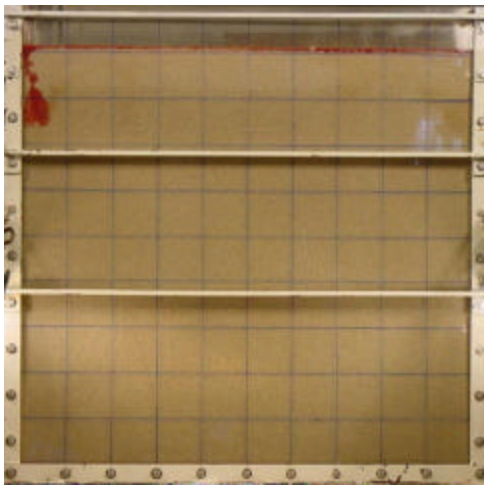

(a) 1st irrigation, *I* = 6mm, *t* = 1 min

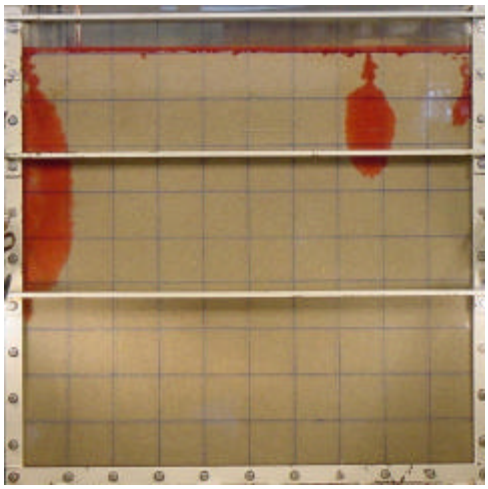

(b) 2nd irrigation, *I* = 6 mm, *t* = 0.5 min

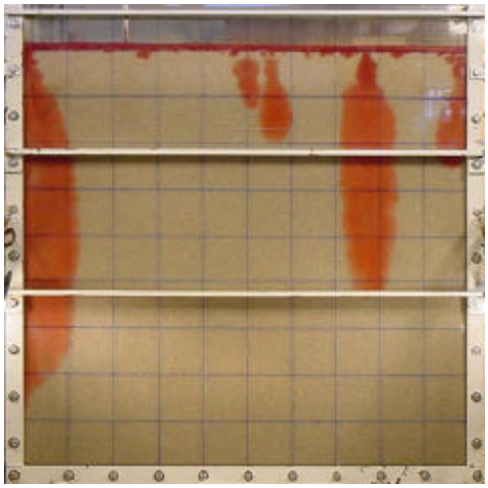

(c) 3rd irrigation, *I* = 6mm, *t* = 17 min

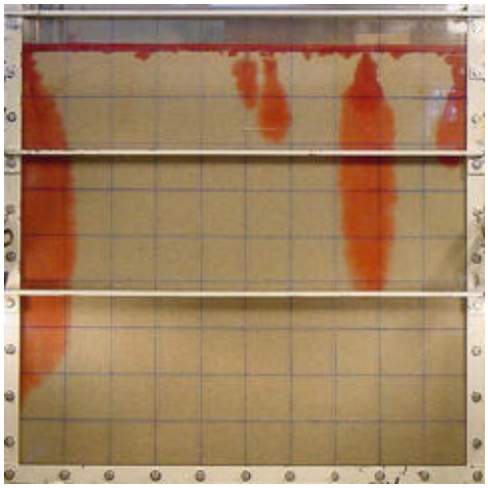

(d) 4th irrigation, *I* = 12 mm, *t* = 3 min

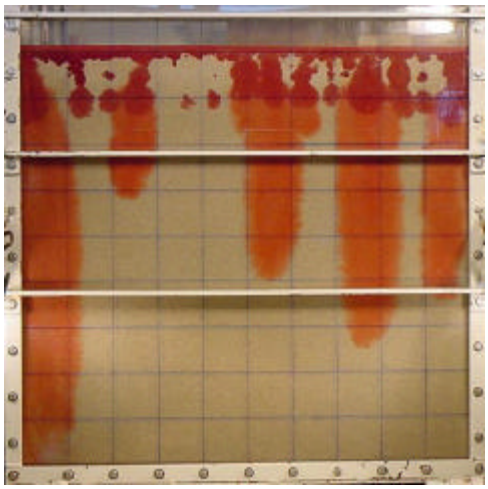

(e) 5th irrigation, *I* = 24mm, *t* = 2 min

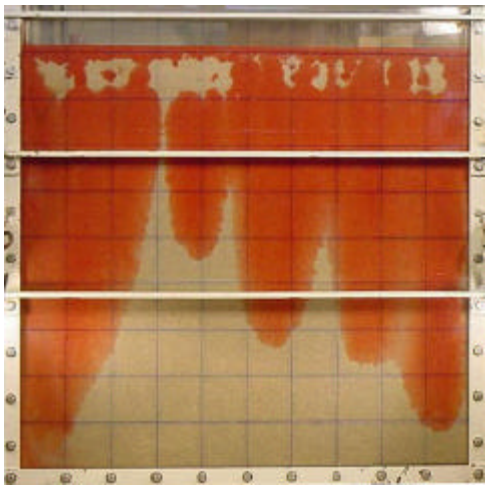

(f) 5th irrigation, *I* = 24mm, *t* = 2 hour

Fig. 8 Redistribution profiles of water in the wet coarse sand with repeated irrigation cycles. The top 10-cm sand was air-dry.